

## ON THE IMPLEMENTATION OF HADAMARD SPECTROSCOPY

Florin GAROI<sup>1</sup>, Petre Cătălin LOGOFĂTU<sup>2</sup>, Iuliana IORDACHE<sup>3</sup>, Tiberius VASILE<sup>4</sup>, Daniela COLȚUC<sup>5</sup>

*In this paper we present the theory of Hadamard spectroscopy and an experimental implementation of it in the visible range of the spectrum, more precisely for the spectrum of a helium lamp. A mechanical mask with 13 elements is used to implement Hadamard spectrometry, resulting in just 7 samples for the recovered spectrum. The advantages and drawbacks of using such a mechanical mask are presented as well as alternatives for improvement.*

**Keywords:** Hadamard spectroscopy, Hadamard transform, mechanical mask.

### 1. Introduction

Nowadays, THz and IR radiation are of great interest for science and technology due to their ability to highlight the complex molecular structure of matter by spectroscopic methods. THz radiation (also known as sub-millimeter radiation) consists of electromagnetic waves in the frequency range 0.1 – 10 THz, and like microwaves, it penetrates a wide range of conductive materials but is partially or totally absorbed by fog, clouds, liquids, or metal.

Regarding THz spectroscopy, there are three established methods: THz Fourier Transform Spectroscopy (THz – FTS) [1 – 4], THz Time-Domain Spectroscopy (THz-TDS) [5 – 9] and Hadamard Spectroscopy (HS) [10 – 15]. The first method is the most common technique used to study molecular resonances. This method uses an interferometric system to investigate a given material. The sample to be analyzed is placed in one of the interferometer optical paths. Usually, with such a technique, a helium cooled bolometer is used as detector and a thermal source as THz generator. The main disadvantages of the THz – FTS method are the limited spectral resolution, only amplitude information from the recorded spectra, and moving parts.

<sup>1</sup> Research scientist, National Institute for Laser, Plasma and Radiation Physics, Romania, e-mail: florin.garoi@inflpr.ro

<sup>2</sup> Research scientist, National Institute for Laser, Plasma and Radiation Physics, Romania, e-mail: petre.logofatu@inflpr.ro

<sup>3</sup> Research scientist, National Institute for Laser, Plasma and Radiation Physics, Romania, e-mail: iuliana.iordache@inflpr.ro

<sup>4</sup> Research scientist, National Institute for Laser, Plasma and Radiation Physics, Romania, e-mail: tiberius.vasile@inflpr.ro

<sup>5</sup> Prof., Research Centre for Spatial Information, University POLITEHNICA of Bucharest, Romania, e-mail: daniela.coltuc@upb.ro

The THz-TDS technique uses a special radiation generation/detection scheme in order to investigate a given sample. Thus, a pulsed laser is used for generation/detection of THz radiation and photoconductive antennae are used as emitter and receiver. The main advantage of this method is the sensitivity to both amplitude and phase of the THz radiation, providing more information than conventional FTS, which is only sensitive to amplitude.

The Hadamard transform, also known as Walsh- Hadamard transform, is an example of a generalized class of Fourier transforms [1]. The spectrometry based on Hadamard class transforms, is a fairly new method. HS has two major advantages: it allows the investigation of weak sources and can be realized without essential moving parts.

This paper presents a HS experiment in the visible range, where the Hadamard type transform is implemented by using a mechanical mask. The paper is organized as follows: Section 2 presents the basics of Hadamard Transform and two other transforms of the same class, Section 3 describes the experimental setup, Section 4 gives some experimental results and Section 5 draws the conclusions.

## 2. Hadamard spectroscopy

Mathematically, the Hadamard spectrometry is a direct and inverse transformation: the spectrum is encoded by a linear binary transform and recovered (decoded) by inverse transformation. The encoding is performed in the optical domain and the decoding in the numeric domain. Between the encoding and decoding positions, a detector is placed that senses the encoded spectrum, sample by sample. The samples are A/D converted and provided to a processor that recovers the initial spectrum.

Fig. 1 shows the main components of HS: the incident spectrally decomposed radiation from the sample is focused (imaged) on a coding mask via the first collecting optics (i.e. a lens or a system of lenses); the mask and the second collecting optics perform the spectrum transformation, and the result is captured and recorded by a detector and further sent to a processor (e.g. computer). The mask is reconfigured for each new sample of the encoded spectrum.

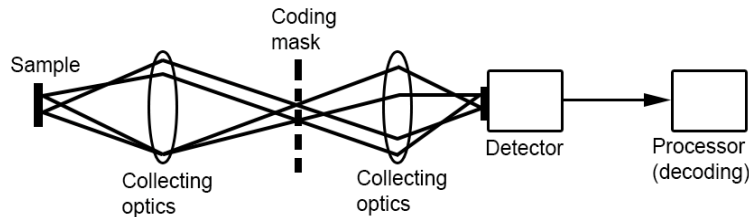


Fig. 1 Diagram of the main components in a Hadamard multiplexing system.

There are two kinds of Hadamard masks: movable (i.e. mechanical) and stationary (i.e. electro-optic) masks. The first ones encode the spectrum by transmitting light while the second ones work by reflecting it. As shown in Fig. 1, the encoding is achieved by transmission. With the mechanical masks, there are no issues related to optical transmission. However, with such systems, the moving parts are prone to mechanical errors. On the other hand, the electro-optic masks have no essential moving parts, but problems due to optical transmission may occur.

## 2.1 Mathematical recipes for Hadamard spectroscopy

There are several transforms that can be used in Hadamard spectrometry. From this class, we briefly present three transforms, with potential in practical applications. The most representative one is the genuine Hadamard transform that gave the name of the technique.

### A. The Hadamard Transform

A linear transform is usually defined by a matrix that has on rows the vectors of the transformed space basis. Supposing that  $H$  is such a matrix, then a spectrum  $S$  is represented by:

$$C = \begin{bmatrix} c_1 \\ c_2 \\ \cdot \\ c_n \end{bmatrix} = HS \quad \text{with} \quad H = \begin{bmatrix} h_1 \\ h_2 \\ \cdot \\ h_n \end{bmatrix} \quad (1)$$

where  $h_i$  are the basis vectors and  $C$  is the spectrum representation in Hadamard space. The elements  $c_i$  are inner products of  $h_i$  and  $S$ .

The Hadamard matrix is obtained by iterating the following equation [16]:

$$H_{n+1} = \begin{bmatrix} H_n & H_n \\ H_n & -H_n \end{bmatrix}, \quad (2)$$

that originates from the single element matrix  $H_0 = [1]$ . The procedure is called *doubling* and allows only the construction of Hadamard matrices of size  $2n$  by using different algorithms, other sizes than  $2^n$  can be obtained [ref].

After detection and A/D conversion, the spectrum is recovered from  $C$  by [16]:

$$S = \frac{1}{N} HC. \quad (3)$$

The masks in Fig. 1 must be configured according to the rows of  $H_n$ , which is a binary matrix, with elements equal to  $+1$  and  $-1$ . The physical implementation of  $-1$  arises some problems because both the transmissive and reflective masks are able to reproduce only the values  $0$  and  $1$ . The solutions are: using two sets of masks (one to insert  $1$ s and the other to insert  $-1$ s), using two detectors, or using an additional mask consisting only of  $1$ s [16]. All of them have the disadvantage of increased complexity and noise, because they involve a

subtraction operation that increases twice the additive noise. For these reasons, other solutions are preferred.

### B. The S Transform

The S transform is an orthogonal transform defined by a binary matrix consisting of 0s and 1s and obtained as follows [16]:

- a Hadamard matrix of the appropriate size is constituted;
- the first row and first column of the matrix are eliminated;
- the -1s are turned into 0s.

The inverse of  $S$  is defined by [16]:

$$S_m^{-1} = \frac{2}{m+1} (2S_m^T - I_m), \quad (4)$$

where  $I_m$  is a matrix with all the elements equal to 1 and  $m$  is the size of the matrix. The  $S$  transform overcomes the implementation problems of Hadamard transform by eliminating the -1 elements.

### C. The Cyclic S Transform

The Cyclic  $S$  is a variant of  $S$  transform. The Cyclic  $S$  matrix can have one of the following sizes [17]:

- $N = 2^n - 1$ ;
- $N = 2t - 1$ ;
- $N = D(D + 2)$ , where  $D$  and  $D + 2$  are prime numbers.

The Cyclic  $S$  matrix is obtained as follows [17]:

- consider a primitive polynomial of order  $n$ :  

$$P(x) = x^n + a_{n-1}x^{n-1} + \dots + a_0$$
- consider the first basis vector and set its first elements to 1:  

$$e_0 = \dots = e_{n-1} = 1$$
- the rest of the elements are obtained with:  

$$e_{m+n} = \sum_{i=0}^{n-1} a_i e_{m+i}$$
- the rest of the vectors are obtained by circular shifts of the first vector (this particularity gives the name of the transform).

The inverse matrix has the same expression as for  $S$  [17]:

$$S_{cyclic}^{-1} = \frac{2}{N+1} (2S_{cyclic}^T - I_N) \quad (5)$$

The Cyclic  $S$  transform is preferred to  $S$  transform due to its cyclic structure that simplifies the control of the masks. This is an important advantage mainly for the mechanical masks where the vectors are chained on a single sliding strip.

## 2.2 Case study: Hadamard spectrum with 7 samples

The resolution of the spectrum measured by Hadamard spectrometry depends on the matrix size. For a 7 samples spectrum, the Cyclic  $S$  matrix must be of size  $7 \times 7$ . Each row corresponds to a mask with 7 binary elements.

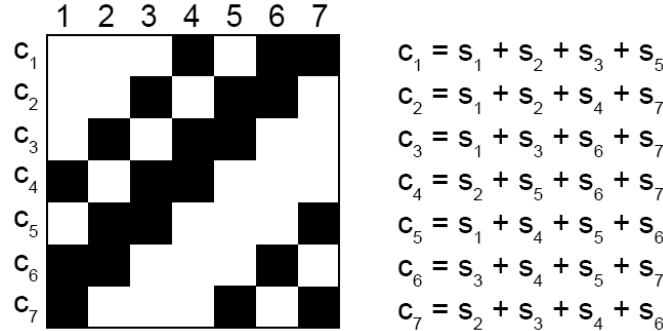


Fig. 2 Graphical representation of a Hadamard matrix, with white and black squares as 1s and 0s, respectively, the equations for the observables.

Fig. 2 shows the set of the 7 masks stacked as in Cyclic  $S$  matrix: the black squares correspond to 0s (light is obstructed) and the white squares to 1s (light is transmitted). The samples of the encoded spectrum are linear combinations of the spectrum samples .

The corresponding sliding strip is shown in Fig. 3. It consists of 7 + 6 elements configured according to the binary sequence (1110100111010). This configuration is used in obtaining the mechanical mask described in Section 3.2.

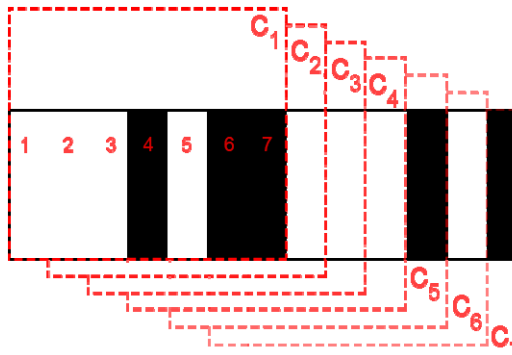


Fig. 3 Graphical representation of a 1D Hadamard matrix, with white and black stripes (i.e. slits or elements) representing a binary system of 1s (i.e. light is passing) and 0s (i.e. light does not pass).

Each consecutive mask is obtained by shifting the window to the right, by one element.

### 3. Experimental setup

#### 3.1 Hadamard spectroscopy with a mechanical mask

For Hadamard spectroscopy, in transmission configuration, we realized the setup in Fig. 4. The radiation from a He spectral lamp is expanded (using a small focal length convex lens and a pinhole or slit) and then collimated with a plane convex lens, such that a wider light beam is sent to the prism. At the exit of the prism, the radiation is decomposed in its spectral components, and projected onto a mechanical mask configured as in Fig. 3. The mask is moved, step by step, such that only 7 elements are illuminated at the moment of sample detection. The masked spectrum is focused by a lens on the detector.

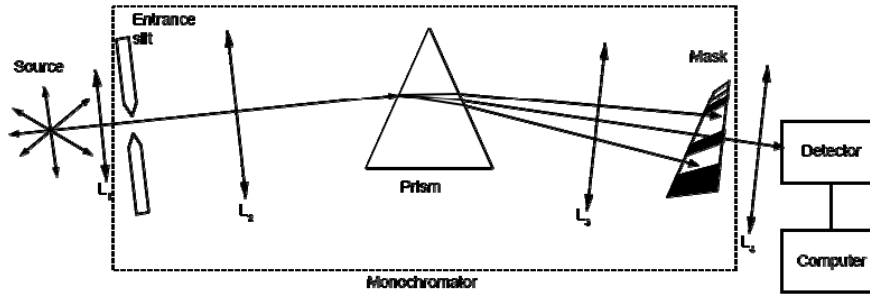


Fig. 4 Transmission Hadamard spectroscopy setup.

#### 3.2 The mechanical mask

The mechanical mask is obtained by cutting slits in a sheet of metal, according to the sequence (1110100111010) (Fig. 5a). A slit is 20mm/2mm (Fig. 6a) in dimension. In order to select a groups of 7 elements, a rectangular window of 20mm/14mm (Fig. 6b) is cut on a second sheet (Fig. 5b).

The window is fixed while the sequence of slits slides behind it and configures, one by one, the rows of the Cyclic S matrix (Fig. 5c). These configurations correspond to the following sequences: (1110100), (1101001), (1010011), (0100111), (1001110), (0011101) and respectively (0111010).

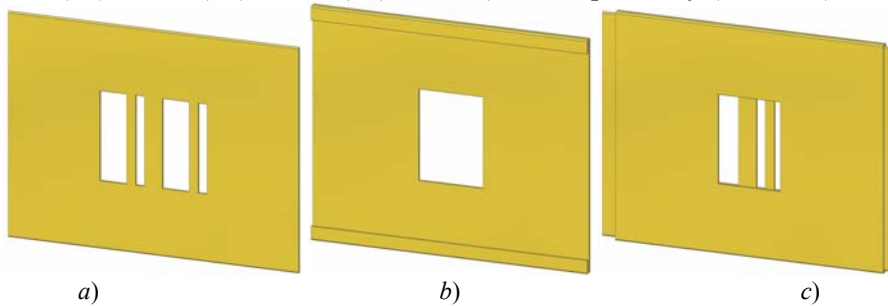


Fig. 5 Mechanical Hadamard mask: a) the 13 elements (transmitting and opaque), b) the window selecting 7 elements at the time, c) the assembled mask.

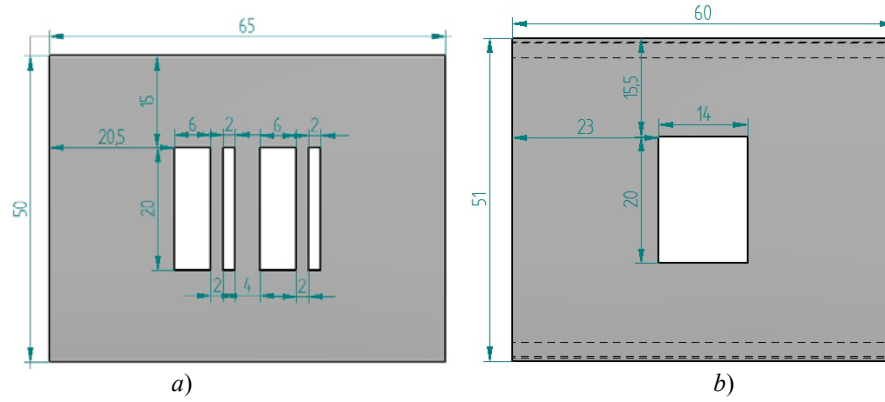


Fig. 6 Hadamard mask components drawings (front view): *a*) the 13 elements, *b*) the window. The last opaque element is not readily noticed as it is part of the opaque surface. From the execution point of view there are only four rectangular cuttings, two of 20 mm  $\times$  6 mm and two of 20 mm  $\times$  2 mm, to make the thirteen elements.

For each configuration, the detector records a voltage value that corresponds to samples  $c_i$ ,  $i = 1, \dots, 7$ . The mask components are made from brass sheets, each with a thickness of 1 mm.

#### 4. Results

For the experiments we used a He lamp as the light source, more precisely, the red and yellow components with wavelengths  $\lambda_{\text{red}} = 7065.71 \text{ \AA}$  and respectively  $\lambda_{\text{yellow}} = 5875.97 \text{ \AA}$  (Fig. 7). With a classic spectrometer, the thinner the slit the higher the resolution and lower the light quantity entering the system.

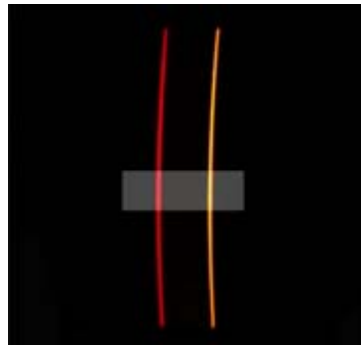


Fig. 7 The two lines in the lamp spectrum obtained with a monochromator. The gray window was used to simulate the low resolution spectrum.

In the case of a Hadamard spectrometer, the resolution is increasing with the number of elements in the mask. Thus, for our 7 elements system, the resolution is quite poor, and the measured spectrum consists in 7 samples. Fig. 8a

shows the result of a first measurement and Fig. 8b the spectrum recovered with eq. (5). Although the plot has only 7 points, two peaks corresponding to the red and yellow spectral lines, mentioned above, are visible. The experiment was repeated three times.

These measured spectra have slightly different shapes due to measuring and mechanical errors [18]. More precisely, the masks were commuted manually and small variations in the position of the slits with respect to the window may cause differences in the recorded voltage values at the detector. The measured intensities also vary with the focal length of the focusing lens on the detector. Thus, the further from the focus the detector is placed the lower the intensity value, recorded as voltage on the detector. This is because the energy of the incident beam is concentrated in a smaller focal spot (i.e. at focus) or in a larger focal spot (i.e. away from focus).

In order to have a reference for our experiment, we simulated the acquisition of the spectrum by taking a snapshot of the spectrum image on a monochromator (Fig. 7).

The image was converted into gray levels and a rectangular area (corresponding to the mechanical mask) was cropped from the centre. The cropped area was split into 7 adjacent rectangles of  $100 \times 44$  pixels, corresponding to the 7 elements of the mechanical mask.

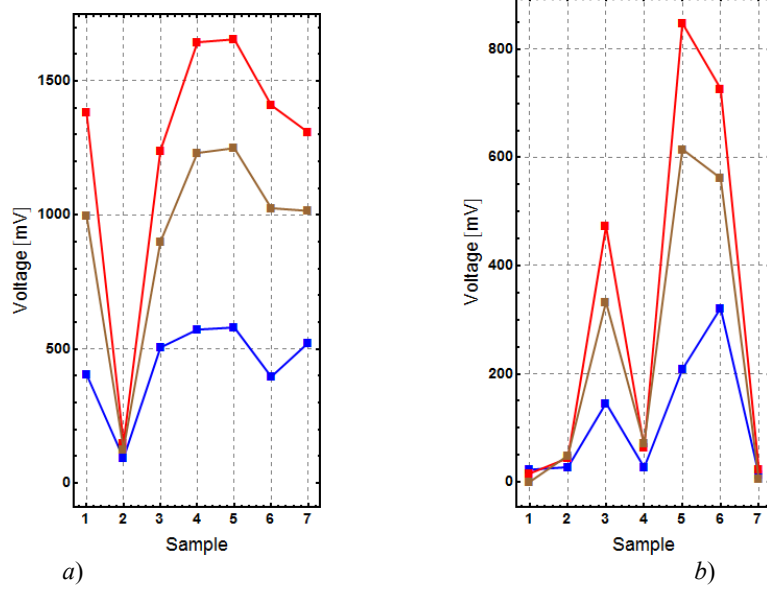


Fig. 8 Results on the two measured spectral lines: *a*) measured values on the detector; *b*) recovered spectra with eq. (5).

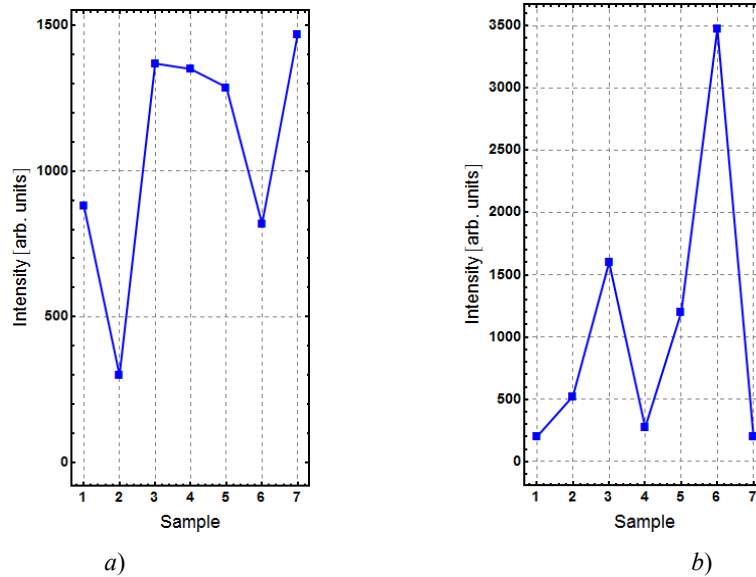


Fig. 9 The simulated spectrum: *a*) the transformed spectrum, *b*) the low resolution spectrum.

By summing the pixels inside each small rectangle, one obtains directly the samples of the low-resolution spectrum, as shown in Fig. 9b. Figure 9a shows the transformed spectrum obtained with eq. (3). As the transformation in HS is done in optical domain, the samples in Fig. 9a are, in fact, the measurements.

## 5. Conclusions

The paper presents some preliminary results regarding the implementation of Hadamard spectrometry. For the first experiment, two spectral lines of a He spectral lamp are considered, namely the red ( $\lambda_{\text{red}} = 7065.71 \text{ \AA}$ ) and yellow ( $\lambda_{\text{yellow}} = 5875.97 \text{ \AA}$ ) lines. A mechanical mask with 13 slits is used to implement the Hadamard spectrometry. With such mask, the recovered spectrum has 7 samples.

Despite the low resolution, the spectral lines are easily distinguished. We may conclude that the mechanical mask has the advantage of a good transmission of radiation. The slightly different patterns of the spectra obtained from repetitive experiments show the presence of errors issued from the mask translation. These mechanical errors and the low resolution of the recovered spectrum are the main disadvantages of the Hadamard spectrometry implementation with mechanical masks.

Following these preliminary measurements, we intend to use a THz - Spatial Light Modulator (THz - SLM) instead of the mechanical mask, in order to eliminate the mechanical errors and to improve the spectrum resolution.

### Acknowledgements

This work was supported by STAR Program of the Romanian Space Agency, project number 17/19.11.2012.

### R E F E R E N C E S

- [1] *J.W. Goodman*, Introduction to Fourier Optics, McGraw-Hill, New York, 1968.
- [2] *Dae-Su Yee, Y. Kim, and J. Ahn*, "Fourier-transform terahertz spectroscopy using terahertz frequency comb", International Quantum Electronics Conference, Lasers and Electro-Optics, IEEE 1-2, 2009.
- [3] *T. J. Parker*, "Fourier transform spectroscopy of solids at terahertz frequencies", Terahertz Science and Technology, **vol. 2**, no. 3, pp. 75 - 89, 2009.
- [4] *J. Dreiser et al*, "Frequency-domain Fourier-transform terahertz spectroscopy of the single-molecule magnet (NEt<sub>4</sub>)[Mn<sub>2</sub>(5-Brsalen)<sub>2</sub>(MeOH)2Cr(CN)<sub>6</sub>]", Chemistry, **vol. 17**, no. 27, pp. 7492 - 7498, 2011.
- [5] *Hans Christian Bakken Skjeie*, Terahertz time-domain spectroscopy, Master of Science in Electronics, Norwegian University of Science and Technology, 2012.
- [6] *M. Naftaly and R. E. Miles*, "Terahertz time-domain spectroscopy for material characterization", Proceedings of the IEEE, **vol. 95**, no. 8, pp. 1658 - 1665, 2007.
- [7] *M. Naftaly et al*, "Terahertz time-domain spectroscopy for textile identification", Applied Optics, **vol. 52**, no. 19, pp. 4433 - 4437, 2013.
- [8] *W. Withayachumankul and M. Naftaly*, Fundamentals of measurement in terahertz time-domain spectroscopy, Journal of Infrared, Millimeter, and Terahertz Waves, Springer Science + Business Media New York, 2013.
- [9] *W. Withayachumankul et al*, "Limitation in thin-film sensing with transmission-mode terahertz time-domain spectroscopy", Optics Express, **vol. 22**, no. 1, pp. 972 - 986, 2014.
- [10] *M. Harwit and N. J. A. Sloane*, Hadamard Transform Optics; Academic Press Inc., New York, 1979.
- [11] *J. Wehlburg et al*, High Speed 2D Hadamard Transform Spectral Imager, Technical report, SAND2002-3846, 2003.
- [12] *Eriks Kupce, Toshiaki Nishida, Ray Freeman*, "Hadamard NMR spectroscopy", Progress in Nuclear Magnetic Resonance Spectroscopy, **vol. 42**, no. 3 - 4, pp. 95 - 122, 2003.
- [13] *Ēriks Kupčē and Ray Freeman*, "Two-dimensional Hadamard spectroscopy", Journal of Magnetic Resonance, **vol. 162**, no. 2, pp. 300 - 310, 2003.
- [14] *Ēriks Kupčē and Ray Freeman*, "Frequency-domain Hadamard spectroscopy", Journal of Magnetic Resonance, **vol. 162**, no. 1, pp. 158 - 165, 2003.
- [15] *Hsueh-Ying Chen and Christian Hilty*, "Hyperpolarized Hadamard spectroscopy using flow NMR", Anal. Chem., **vol. 85**, no. 15, pp. 7385 - 7390, 2013.
- [16] *N. Sloan*, "Multiplexing methods in spectroscopy", Mathematics Magazine, **vol. 52**, no. 2, pp. 71 - 80, 1979.
- [17] *E. D. Nelson*, "Hadamard spectroscopy", Journal of the Optical Society of America, vol. 60, no. 12, pp. 1664 - 169, 1970.
- [18] *M. H. Tai, M. Harwit, and N. J. A. Sloane*, "Errors in Hadamard spectroscopy or imaging caused by imperfect masks", Applied Optics, **vol. 14**, no. 11, pp. 2678 - 2684, 1975.